

# Detailed Modeling of Biomass Gasification in Dual Fluidized Bed Reactors under Aspen Plus

L. Abdelouahed, O. Authier,<sup>†</sup> G. Mauviel, J. P. Corriou, G. Verdier, and A. Dufour\*

CNRS, Laboratory of Reactions and Process Engineering, ENSIC, 1, Rue Grandville, BP 20451, 54001 Nancy Cedex, France

## Supporting Information

**ABSTRACT:** The modeling of biomass gasification processes by simulators such as Aspen Plus is a powerful tool to assess mass and energy balances and to optimize process designs. A detailed model of the gasification reactor is one of the key points to achieve an accurate process description. A model for biomass gasification in dual fluidized bed (DFB) reactors by coupling Aspen Plus and dedicated Fortran files is presented. The DFB is divided into three modules according to the main chemical phenomena: biomass pyrolysis, secondary reactions, and char combustion. Mass yields of permanent gases, water, 10 tar species, and char are modeled with respect to the reactor temperature by a pyrolysis correlation. The secondary reactions are modeled by a semidetained kinetic mechanism that handles gas-phase and catalytic conversions over char of CH<sub>4</sub> and lumped tar species (phenol, naphthalene, benzene, and toluene), gas-phase water–gas shift reaction (WGSR), char, and soot–steam gasification. The calculated compositions of permanent gases and tars, flow rates, and lower heating values are compared with experimental data for two DFB technologies (Tunzini Nessi Equipment Companies (TNEE) and Battelle High Throughput Gasification Process (FERCO)). The syngas composition and flow rate are very sensitive to the WGSR kinetic. The rate laws for WGSR are reviewed. An optimized kinetic law for WGSR is given.

## 1. INTRODUCTION

Lignocellulosic biomass is a promising fuel resource: it is well-spread worldwide and close to be carbon neutral. Its solid state and its low energetic content imply local utilization such as domestic heating and cooking. Besides solid fuel gasification allows the production of syngas (CO + H<sub>2</sub>). After tar abatement and other purification steps, syngas could be converted into heat and power (CHP), Fischer–Tropsch diesel, synthetic natural gas (SNG), methanol, etc. Electricity and/or fuels are better energy carriers than solid biomass itself. Nevertheless, biomass gasification is not a mature technology. There are only few commercial scale gasifiers (dual fluidized bed (DFB) at Güssing in Austria,<sup>1</sup> entrained flow reactor for Choren in Germany,<sup>2</sup> etc.). To spread and improve gasification processes, engineers should be able to model mass and energy balances for any gasification processes with more confidence than they are able to do today. This is especially the case for processes based on DFB.

DFB used for gasifying biomass with steam or recycled gas is considered to be a promising technology to produce a high-quality gas (mainly CO and H<sub>2</sub>) without dilution in nitrogen. The concept emerged in the 1970s from pioneering studies conducted by Battelle Columbus (United States).<sup>3</sup> An increasing number of research programs have been dedicated to biomass DFB all over the world, and the concept is nowadays a viable industrial solution.<sup>1,4,5</sup> Generally, the process includes two reactors in series with circulation of hot fluidizing particles (see Table 1): a gasification reactor (gasifier), inside of which biomass is fed and syngas exits from the top, and a combustion reactor (combustor), where the outlet stream is carbon dioxide, steam, and ash. Combustion of residual char and of additional fuels inside the combustor provides the heat

required for the endothermic reactions occurring in the gasifier.<sup>6</sup>

To compare the efficiency and selectivity of different gasification processes, process simulators such as Aspen Plus,<sup>7–16</sup> Simulink,<sup>17</sup> and Cycle-Tempo<sup>18</sup> are used. The modeling of biomass gasification processes with such software is a powerful tool to evaluate mass and energy flows and to perform further economic and environmental evaluations for different processes designs. A detailed modeling of the gasification reactor is one of the key points to achieve a realistic process description.

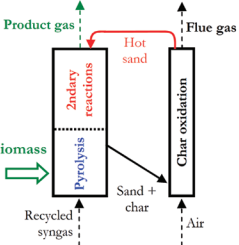
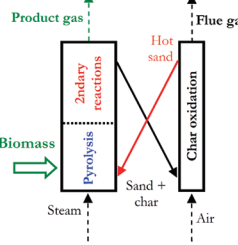
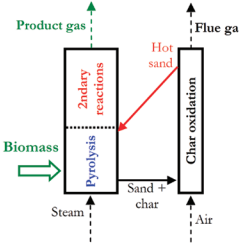
The composition and yields of the gasifier's products are more often modeled (i) by considering thermodynamic equilibrium (by minimizing the Gibbs free energy),<sup>17,19</sup> (ii) by using two equilibrium reactors in series with a selective bypass over the first one,<sup>18</sup> or (iii) by breaking up biomass into its constituting elements (C, H, N, O, S, Cl, ash, and moisture) and dealing with them separately.<sup>11,15,16</sup> Nevertheless, the decomposition of biomass into its elements does not account for the true phenomenological mechanisms. Indeed, biomass is first decomposed by pyrolysis reactions, and the products yields are more often controlled by kinetic limitations and not by thermodynamic equilibrium, unless reactor temperatures are very high (>1400 °C) or very active catalysts are used.<sup>20</sup> Models based on thermodynamic equilibrium fail to take into account the multistep physical and chemical phenomena occurring in the gasifier. Among other substantial deviations from experimental data, methane and tar contents in the

**Received:** March 7, 2012

**Revised:** May 1, 2012

**Published:** May 1, 2012

Table 1. Simplified Scheme and Description of Three Complementary Technologies of DFB Gasifier<sup>a</sup>

Name of the technology	TNEE 30, 36, 37	FERCO 3, 31	Güssing 32, 33
Development beginning	In the 1980's	In the 1970's	In the 1990's
Simplified scheme			
Description	Gasification: Low Velocity Fluidized Bed (LVFB) Char oxidation: High Velocity Pneumatic Riser (HVPR). The hot bed material is injected to the top of the pyrolyser. Better gas/solid contact between the pyrolysis gas and the hot sand from combustion due to the "Saturne" contactor.	Gasification: HVPR Char oxidation: HVPR. Due to HVPR gasification the solid residence time is low and incomplete pyrolysis conversion could be achieved.	Gasification: LVFB. Char oxidation: HVPR. The hot bed material is injected to the middle of the gasifier. Little hot catalyst is present in the freeboard of the gasifier.
Technology definition (see text for the definition of the $Y_i$ )	$Y_1=0.05$ , $Y_2=0$ , $Y_3=1$ , $Y_4=1$	$Y_1=0$ , $Y_2=1$ , $Y_3=0$ , $Y_4=0$	$Y_1=0.05$ , $Y_2=0$ , $Y_3=0$ , $Y_4=0$

<sup>a</sup>Biomass introduced by screw conveyors for all technologies.

product gas and the unconverted carbon in the solid phase are underpredicted by thermodynamic equilibrium.<sup>20,21</sup>

Another possible approach is to model the gasifier by empirical correlations based on data collected from a specific gasifier plant.<sup>8,12</sup> This method is thus very convenient, but only to simulate the gasifier technology corresponding to the collected data. Such correlations cannot be easily extended to other technologies.

Some extensive works<sup>9,13,14</sup> proposed to decompose the gasifier in reaction modules such as pyrolysis of biomass (or "devolatilization") and combustion of char. The yields and compositions of biomass pyrolysis products are computed from correlations based on experimental mass balances or from a detailed chemical modeling (not directly implemented in Aspen).<sup>13</sup> Pyrolysis products (gas, tar, and char) were considered as feeds to other reactors. Gas and tar were sent to a gaseous products conversion reactor, while char was oxidized in a combustor; both were modeled as Gibbs reactors<sup>14</sup> or with a kinetic approach.<sup>13</sup> Despite these extensive works, the main chemical mechanisms, including a semidetailed kinetic mechanism for tar conversion, have never yet been implemented under Aspen Plus for modeling biomass gasification in DFB.

The authors are aware that many modeling approaches of fluidized beds have been developed taking into account the hydrodynamic's effect to describe biomass gasifiers,<sup>11,22–25</sup> but reactor performances in terms of feedstock conversion and product composition also greatly depend on reaction rates.<sup>21,26</sup>

The aim of this paper is not to describe the detailed hydrodynamics of the fluidized bed but rather to give a methodology to include detailed chemical mechanisms in process simulators without any thermodynamic equilibrium assumptions.

Gasification reactors are modeled by coupling Aspen Plus and dedicated Fortran files. The main chemical phenomena are decoupled and a semidetailed kinetic approach is used, including tar catalytic conversion. The calculated compositions of permanent gases and tar, their mass yields, and lower heating values (LHV) are compared with experimental data for two DFB technologies.

## 2. DFB MODELING USING ASPEN PLUS

**2.1. Presentation of the Different Technologies of DFB.** Depending on the technology of the DFB, the gasifier and the combustor can be a dense fluidized bed or a pneumatic riser. Xu et al.<sup>9,16,27–29</sup> presented in an extensive work four combinations of DFB depending on the fluidization regime of the 2 reactors (gasifier and combustor). It has been demonstrated that the best technical choice for a DFBG is gasification into a dense low velocity fluidized bed (LVFB) and char combustion into a high velocity pneumatic riser (HVPR). Other options were not taken into account in this work.<sup>9,16,27</sup> The DFB technology can also depend on the level of the hot sand injection from the combustor to the gasifier. Indeed, the hot sand could be injected to the bottom, middle, or top of the FB gasifier.

Table 1 displays three different technologies of DFB, complementary of those proposed by Xu et al.<sup>27</sup> Staged gasification with a third FB following the approach of Dong et al.<sup>29</sup> is out of the scope of the present paper.

The TNEE process<sup>30</sup> has been developed in France in the 1980s in collaboration between TNEE company and Nancy and Compiègne universities. In this process (see Figure S.1 in Supporting Information and Table 1), the gasifier is a LVFB and the combustor is a HVPR. The sand is injected to the top of gasifier through a staged distributor (the "SATURN" technology). The SATURN technology is a gas/solid contactor that allows a good distribution of the hot sand flow. The intense contact between the hot sand at counter-current with the pyrolysis gas is thought to achieve a higher tar cracking. The pyrolysis FB was fluidized by recycling a fraction of the produced syngas ( $\approx 14$  mass % of the product cleaned syngas was recycled). This process was operated during more than 2000 h at 500 kg/h (on fir bark). It has been dismantled because of a too low fossil fuel cost and has been then almost "forgotten" by the biomass community until the review by Corella et al.<sup>4</sup>

In the FERCO gasification process,<sup>3,31</sup> the gasifier and the combustor are two HVPRs. The hot sand from the combustor is injected to the bottom of the gasifier. The gasifier is fluidized by steam.

In the Güssing process,<sup>1,32,33</sup> the gasifier is a LVFB and the combustor is a HVPR. This technology is currently one of the most advanced from an industrial point of view. It is quite close to those previously developed in China in the 1990s.<sup>34</sup> Calcinated olivine is used as the catalytic bed material and injected to the middle of the gasifier fluidized by steam. The general idea of using bed material for both heat transfer and chemical interaction with the gas phase from intensive contact in the top section of the LVFB is currently studied in order to improve the Güssing classical design where the solids' concentration approaches zero in the freeboard zone.<sup>35</sup>

In this paper, only the modeling of FERCO and TNEE technologies are presented.

**2.2. A Decoupling Methodology.** In the present study, the Aspen Plus process simulator was selected to develop the model of the gasifier. It allows the modeling, design and process optimization in steady state. It has large databases of physical properties and thermodynamic models. The presented methodology could be extended to other process simulators, but Aspen Plus was chosen mainly because of its better database for unconventional solids and the pioneering work of the NREL.<sup>7,8</sup> The chemical species are transformed by a series of unit operations connected by flows of materials or heat.

Aspen Plus has the flexibility to allow the insertion of Fortran blocks.<sup>38</sup> This feature is used for the integration of complex reactor models that are not available in Aspen predefined blocks. It is also used for compiling the library files in the definition of unconventional components, such as biomass, char, etc. (molecular weight, density, heat capacity, etc.).<sup>7,8,39</sup>

The detailed model of the reactor is achieved in different Fortran files coupled to Aspen by means of dll files. An Intel Fortran 9.0 compiler is used to compile Fortran files. This coupling method is different from the Fortran calculators embedded in Aspen. The embedded calculator was tested but did not achieve stable results, especially when iterations between enthalpy balances (by Aspen) and mass balances (by Fortran) are needed.

Reactor inlets (mass and enthalpy flow rates), temperature, and pressure (etc.) are transferred from Aspen to Fortran files, which allows reactor modeling implementation by means of empirical correlations (product yields as a function of temperature), chemical kinetics, or more detailed reactor computations. Results from Fortran calculations (product mass flow rates, etc.) are then transferred to Aspen (Figure 1). Iterations occur between Aspen (temperature calculated by enthalpy balance) and the Fortran file (mass balance calculated using the temperature from Aspen).

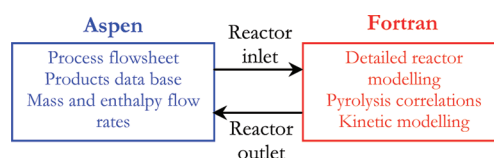


**Figure 1.** Principle of coupling Aspen Plus flowsheet with external Fortran files.

None of the commercial process simulators (Aspen plus, ProII, Hysys, etc.) have predefined models to simulate biomass gasification in dual fluidized bed reactor. A new model has thus been developed that is based on decoupling of the main chemical phenomena (Figure 2).

Our approach is close to those adopted by Sadhukan et al.<sup>14</sup> and Biagini et al.,<sup>13</sup> but a more detailed kinetic scheme with lumped tar species and catalytic conversion of these species (see section 2.3.) is implemented under Aspen Plus. It is a useful tool to improve prediction of reactor behavior and gas composition with basic assumption of ideal hydrodynamics. Biomass particle residence time is most of the time long enough in LVFB to achieve a complete pyrolysis.<sup>26,40–42</sup> Consequently, the apparent rate of pyrolysis, which depends on a complex coupling among bed hydrodynamic, external and internal (inside the particle) heat transfers, and intrinsic pyrolysis chemical kinetic,<sup>43</sup> does not need to be modeled for our purpose (modeling of product composition under Aspen). Pyrolysis is assumed to be complete and to occur in a perfectly stirred reactor (PSR) inside the solid bed material. In the dense bed of FB, gas bubbles formed after the distributor rise in the bed and exchange heat and mass with the solid particle.<sup>44,45</sup> In principle, the dense phase is simulated as a PSR, whereas the bubble phase is simulated as a plug flow reactor.<sup>22</sup> Nevertheless, it was previously shown that biomass pyrolysis mainly occurs at the splash zone.<sup>40</sup> In the present study, the bubble phase has been thus neglected, because the pyrolysis vapors are assumed to be released only from the splash zone. They are released from the splash zone to the freeboard that is modeled by a plug flow reactor, as generally assumed.<sup>22,26</sup> The char produced from biomass pyrolysis is assumed to be steam gasified in the dense phase simulated as a global PSR and then also in the freeboard (if entrained). The residence time of the char entrained to the freeboard is assumed to be equal to the residence time of gases ( $\tau$ ) in the freeboard.

Many advanced models<sup>24,44,46,47</sup> were developed for FB hydrodynamic, but a detailed hydrodynamic model of fluidization is not the aim of this paper.

The DFB reactors are described by a general scheme (see Figure 2) that can represent all technologies of DFB, depending on the mass flow rate ratios  $Y_1$ ,  $Y_2$ ,  $Y_3$ , and  $Y_4$ , defined as follows:

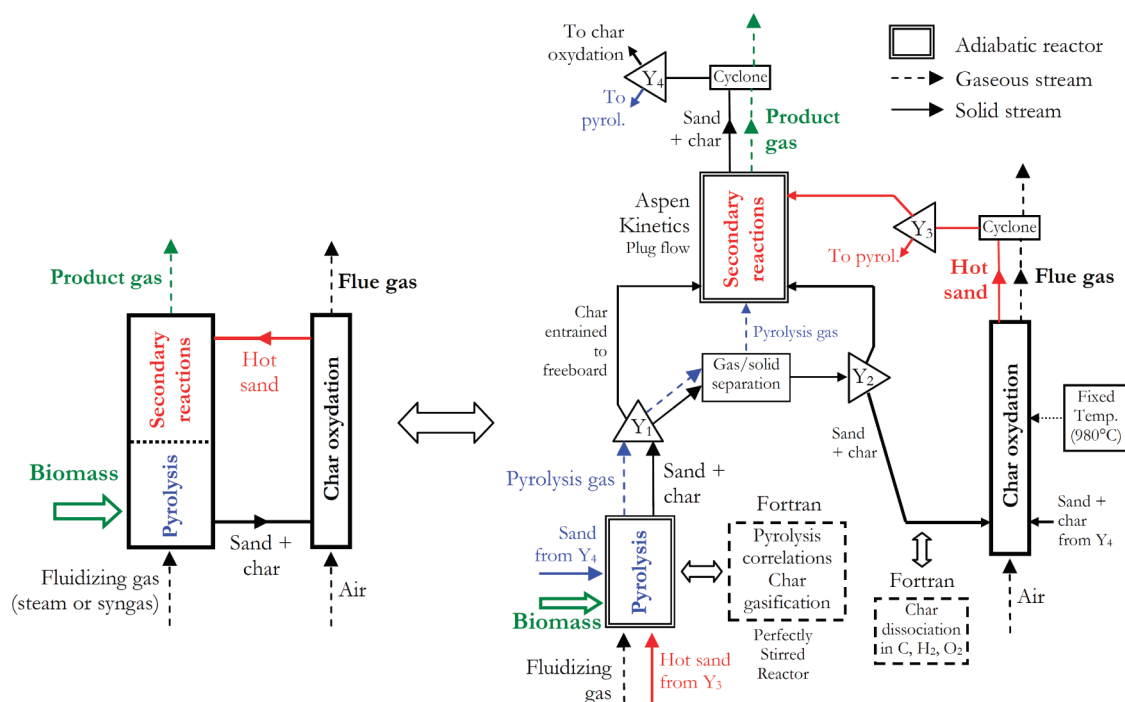


**Figure 2.** Simplified scheme of the model developed under Aspen Plus for biomass gasification in different dual fluidized bed technologies (see Table 1 for more details about the technologies).

$$Y_1 = \frac{\text{char entrained to secondary react. zone flow rate}}{\text{total char produced flow rate}} \quad (1)$$

When  $Y_1$  is high, the majority of char produced by the pyrolysis is entrained from a LVFB to the freeboard. This ratio  $Y_1$  is useful only when  $Y_2$  is not set to 1.

$$Y_2 = \frac{\text{sand + char to the secondary react. zone}}{\text{total sand + char flow rate after pyrol. gas/solid sep.}} \quad (2)$$

When  $Y_2$  is high, the solid (char + sand) from the pyrolysis zone is directly entrained to the secondary reactions zone, as in the FERCO reactor, in a high velocity gasification fluidized bed, but unlike in the Güssing or TNEE process (see Table 1).

$$Y_3 = \frac{\text{hot sand to secondary react. zone}}{\text{total hot sand at outlet of combustion}} \quad (3)$$

When  $Y_3$  is high, the hot sand from the combustion zone is directly introduced in the secondary reaction zone by the top of the gasification FB, as in the TNEE process. If it is low, the hot sand is injected in the bottom part of the gasification FB (as in the Güssing or FERCO processes).

When  $Y_2$  and  $Y_3$  are low (like in the Güssing process), the secondary reaction zone (freeboard) has low mass fraction of sand/catalyst coming only from entrainment by the gases from the pyrolysis low velocity fluidized bed.

$$Y_4 = \frac{\text{sand entrained in pyrolyzer from secondary react. zone}}{\text{sand outlet from secondary react. zone}} \quad (4)$$

When  $Y_3$  and  $Y_4$  are high, the hot sand goes from the combustor to the zone of secondary reactions, then to pyrolysis. The sand falls counter-currently with respect to the pyrolysis gas flow (see TNEE process, Table 1 and Supporting Information).

The  $Y_i$  values for the main DFB technologies are given in Table 1.

**2.3. Chemical Reactions Implemented in the Aspen–Fortran Model.** The chemical reactions occurring in the three decoupled zones of the reactors (see Figure 2) are the following: pyrolysis and char steam gasification, and secondary reactions and char oxidation by air. Table 3 summarizes all the reactions implemented in the model. The units were converted in the international system (in kmole, kg, Pa, m<sup>3</sup>, s, kJ, and K).

The term “secondary reactions” has a different meaning in this paper with regard to the one defined by Milne and Evans.<sup>48</sup> The “secondary reactions” included in the present model are water–gas shift reaction (WGSR), gas-phase and catalytic conversion of tars over char, catalytic conversion of methane over char, and char and soot gasification. They were selected from our background of chemical mechanisms occurring in DFB<sup>43</sup> and are in agreement with ref 26.

Char–steam gasification kinetic is handled by the model both in the dense bed (PSR for the solid) and in the freeboard (plug flow of the char entrained in the freeboard).

**2.3.1. Pyrolysis Products Yield.** The correlations of pyrolysis give the mass fractions of the pyrolysis products as a function of the temperature of the gasification reactor. This temperature is not the temperature of particles primary pyrolysis but of the sand. These correlations include biomass primary pyrolysis and primary tar conversion (that is very fast at gasifier temperature) to simplify the model. The primary tars are composed of more than one hundred different species, and their yields of formation and conversion are not yet known. Our pyrolysis correlation is thus a simplified method to give the yield of pyrolysis products including the major secondary/tertiary tars.

These correlations were determined by previously described experiments and detailed tar analysis.<sup>49–51</sup> They are suitable for reactor temperatures between 700 and 1000 °C and for average particles heating rates (see ref 50 for the definition of the heating rates) between 20 and 40 °C/s. Such heating rates are currently achieved in fluidized bed reactors with wood chips of



around 5 mm thickness.<sup>50,52</sup> Consequently, they are suitable for FERCO and TNEE gasifiers.

The correlations used give the mass yields of the main permanent gases (CO, H<sub>2</sub>, CO<sub>2</sub>, CH<sub>4</sub>, C<sub>2</sub>H<sub>4</sub>, C<sub>2</sub>H<sub>6</sub>), water, and 10 tars species (benzene, toluene, *o*-xylene, phenol, indene, cresols, naphthalene, 1+2methylnaphthalene, acenaphthylene, and phenanthrene).

To simplify the model, the 10 tars species are lumped into 4 groups:

- “benzene” = benzene
- “phenol” = phenol and cresols,
- “toluene” = toluene, xylene, and indene
- “naphthalene” = naphthalene, 1+2methylnaphthalene, acenaphthylene, and phenanthrene.

Benzene, phenol, toluene, and naphthalene are defined as the model compounds of these four tars “lumped” species.

The parameters *a*, *b*, and *c* of the correlations for the mass yields of the pyrolysis products are given in Table 2.

**Table 2. Parameters for the Correlations of Pyrolysis<sup>50,51,a</sup>**

product	<i>a</i>	<i>b</i>	<i>c</i>
CH <sub>4</sub>	$-4.341 \times 10^{-5}$	$10.12 \times 10^{-2}$	-51.08
H <sub>2</sub>	$1.362 \times 10^{-5}$	$-2.517 \times 10^{-2}$	12.19
CO	$-3.524 \times 10^{-5}$	$9.770 \times 10^{-2}$	-24.93
CO <sub>2</sub>	$3.958 \times 10^{-5}$	$-9.126 \times 10^{-2}$	64.02
C <sub>2</sub> H <sub>4</sub>	$-6.873 \times 10^{-5}$	$14.94 \times 10^{-2}$	-76.89
C <sub>2</sub> H <sub>6</sub>	$8.265 \times 10^{-6}$	$-2.105 \times 10^{-2}$	13.38
C <sub>6</sub> H <sub>6</sub>	$-3.134 \times 10^{-5}$	$7.544 \times 10^{-2}$	-42.72
C <sub>7</sub> H <sub>8</sub>	$-4.539 \times 10^{-6}$	$0.687 \times 10^{-2}$	1.462
C <sub>6</sub> H <sub>6</sub> O	$1.508 \times 10^{-5}$	$-3.662 \times 10^{-2}$	22.19
C <sub>10</sub> H <sub>8</sub>	$-8.548 \times 10^{-6}$	$1.882 \times 10^{-2}$	-9.851
H <sub>2</sub> O	$5.157 \times 10^{-5}$	$11.86 \times 10^{-2}$	84.91

<sup>a</sup>Mass yields (*Y<sub>i</sub>*, based on anhydrous biomass) of pyrolysis products are calculated as a function of the sand temperature (in Kelvin) in the pyrolysis zone, assumed as a PSR (see text) as  $Y_i = aT^2 + bT + c$ .

Char mass yield is calculated by difference in the Fortran file after other products determinations by the correlations to perfectly closed the mass balance. Char mass yield (based on anhydrous biomass) was 16.2% for TNEE process (pyrolysis reactor at 760 °C). Our model takes also into account the variation of char elemental composition upon the pyrolysis reactor temperature to give more detailed mass and enthalpy balances. The evolution of the elemental composition of char depending on the reactor wall temperature is taken from ref 50, given in Table S.1 (Supporting Information), and calculated from the Fortran file also used for the mass yield correlations.

**2.3.2. Kinetics of Secondary Reactions.** In this study, the catalytic cracking of CH<sub>4</sub> over char<sup>53</sup> and the tar gas phase<sup>54,55</sup> and catalytic cracking over char<sup>56,57</sup> are considered (see Table 3 and the Supporting Information). Gas phase conversion of CH<sub>4</sub> is known to be negligible under the studied conditions.<sup>20</sup> There is a lack in kinetic data about the catalytic effect of sand (assumed as pure SiO<sub>2</sub>) or other bed material, and the sand is usually assumed to be chemically inert.

Char entrained with the sand may have a catalytic effect on tar<sup>56,57</sup> and methane conversion.<sup>58</sup> The heterogeneous cracking of benzene and toluene over char is assumed to be similar to naphthalene due to a lack of kinetic data, but toluene should be more reactive (giving benzene and CH<sub>4</sub>) than unsubstituted aromatics.<sup>54</sup> The calculation of the kinetic constants is detailed

in the Supporting Information. The thermal and catalytic conversion of C<sub>2</sub> compounds over char is neglected also because of a lack of kinetic data.

**2.4. Definition of ASPEN Plus Modeling.** **2.4.1. Reactor Parameters Inputs.** To compare the model with experimental data, the same input parameters were set between the model and the pilot plants operating conditions. Table 4 gives the main operating inputs for FERCO and TNEE flow sheets.

The biomass flow rate is assumed as 1 kg/s of anhydrous biomass. This scale is in accordance with the technico-economic feasibility of DFB reactors.<sup>66</sup>

Because the gasifier in FERCO is a HVPR, the volume of the secondary reaction zone is assumed to be equal to the volume of the reactor. The pyrolysis is thus assumed to occur in a small volume of the reactor. This assumption leads to an overestimation of the “effective” volume of the secondary reactions zone.

The TNEE gasification reactor is a LVFB with a freeboard section for secondary reactions. The volume of the freeboard only is thus taken for secondary reactions, in accordance with Bruni et al.<sup>40</sup> who showed that pyrolysis could occur at the splash zone thus leading to few secondary reactions in the dense bed.

**2.4.2. Definitions of Components, Biomass, and Char.** To define the different components, the function MIXCINC meaning “conventional components, conventional solids, and non-conventional components without size distribution” is chosen as current type.

The RK-Aspen (Redlich–Kwong–Aspen) equation of state is recommended for hydrocarbon processing applications, such as gas-processing, refinery, and petrochemical processes.<sup>38</sup> It is used to calculate thermodynamic properties of conventional components.

Biomass and char are defined in Aspen Plus as a nonconventional solid. HCl1Boie method is used to calculate the enthalpy of biomass and char by using Boie’s correlations<sup>62</sup> based on proximate and ultimate analyses (see Table 5 for wood composition and Table S.1. in the Supporting Information for char composition). Only carbon, hydrogen, and oxygen are considered in the ultimate compositions of biomass and char. Nitrogen and sulfur compositions of biomass and char are neglected in this paper.

Biomass and char densities are calculated by the DCOALIGT method<sup>8</sup> using IGT’s<sup>38</sup> correlations, on the basis of the ultimate analysis.

We noticed a significant difference between the char heat capacity and density calculated by Aspen Plus and their respective experimental values. Consequently, the heat capacity and density of char were modified. The Raznjevic et al.<sup>63</sup> correlation is used to calculate the heat capacity of char (relation 5), and the density is set to 170 kg/m<sup>3</sup>.<sup>64</sup>

$$C_p = 419.96 + 2.09T - 6.85 \times 10^{-4}T^2 \quad (\text{J}/(\text{kg K})) \quad (5)$$

Sand (assumed as a pure SiO<sub>2</sub>) is defined as a conventional solid component without size distribution.

**2.4.3. Operating Blocks and Flow-Sheet.** The Aspen flow sheet for TNEE process is given in Figure 3. The flow sheet for FERCO process is given in the Supporting Information.

The streams and operation units used in the model are presented in Tables 6 and 7, respectively.

Heat losses are assumed to be negligible in all operation units. Energy streams presented in Table 6 and Figure 3 are not

Table 3. Reactions Implemented in the Aspen–Fortran Model (in kmole, kg, Pa, m<sup>3</sup>, s, kJ, and K)

reactor zone	reaction	rate law (kmol/(m <sup>3</sup> s))	ref	assumptions
pyrolysis zone	pyrolysis correlations	Mass yield ( $Y_i$ ) of products as a function of reactor temp. in the form $Y_i = aT^2 + bT + c$ with $a$ , $b$ , $c$ coefficients optimized from experimental results	S0, S1	Heat transfers are not modeled. No kinetic modeling of the solid pyrolysis.
char gasification	$C_xH_yO_z + (x - y)H_2O \rightarrow xCO + (x - z + \frac{y}{2})H_2$	$r_1 = 4.8 \times 10^4 \exp\left(-\frac{211000}{RT}\right) p_{H_2O}^{0.51}$	S9	Reaction in a perfectly stirred reactor (dense bed) under Fortran. Residence time varies from one technology to another.
secondary reactions zone	homogeneous (gas-phase) reactions	$r_2 = 3.4 \times 10^{14} \exp\left(-\frac{350000}{RT}\right) C_{C_{10}H_8}^{1.6} C_{H_2}^{-0.5}$ $r_3 = 4 \times 10^{16} \exp\left(-\frac{443000}{RT}\right) C_{C_6H_6}^{1.3} C_{H_2}^{-0.4} C_{H_2O}^{0.2}$ $r_4 = 1.04 \times 10^{12} \exp\left(-\frac{247000}{RT}\right) C_{C_7H_8}^{0.5} C_{H_2}^{0.5}$ $r_5 = 10^7 \exp\left(-\frac{10^5}{RT}\right) C_{C_6H_6O}$ $r_6 = 1.2 \times 10^{10} \exp\left(-\frac{318000}{RT}\right) C_{H_2}^{0.5} C_{CO_2}$	S4	Reactions occur in a PFR. Residence time of gas ( $\tau$ ) is calculated by Aspen and depends on the reactor vol. and temp. The stoichiometry for tar conversion reactions are from this work and are only a first assumption based on the experimental data from the referenced papers. No kinetics data is available for $C_6H_6$ and $C_7H_8$ catalytic conversion over char. The kinetics laws were thus assumed from $C_{10}H_8$ , although $C_6H_6$ should be less reactive and $C_7H_8$ more reactive than $C_{10}H_8$ . Char concn is taken into account in the pre-exponential factor of reactions 8–10, and 12 (see Supporting Information). The kinetic of water–gas shift was reviewed (see text and appendix 1). The work of Bustamante et al. <sup>61</sup> was chosen because the kinetic law matches with the prediction of a detailed kinetic mechanism developed at CNRS. <sup>20</sup> The pre-exponential factors were optimized and matched to be the same for both technologies.
	$CO_2 + H_2 \rightarrow CO + H_2O$	$r_7 = k_7^0 \exp\left(-\frac{102400}{RT}\right) C_{H_2O} C_{CO}$ with $k_7^0 = 1.35 \times 10^5$ from ref 61 $k_7^0 = 5.2 \times 10^5$ optimized	60	
	$CO + H_2O \rightarrow CO_2 + H_2$	$r_8 = 21.11 \exp\left(-\frac{61000}{RT}\right) \frac{m_{char}}{V_R} C_{C_{10}H_8}$	S7	61, and kinetic constant optimized
heterogeneous catalytic conversion over char	$C_{10}H_8 \rightarrow 9C + \frac{1}{6}C_6H_6 + \frac{7}{2}H_2$	$r_9 = 21.11 \exp\left(-\frac{61000}{RT}\right) \frac{m_{char}}{V_R} C_{C_6H_6}$	assumption adapted from ref S7	
	$C_6H_6 + H_2O \rightarrow 3C + 2CH_4 + CO$	$r_{10} = 21.11 \exp\left(-\frac{61000}{RT}\right) \frac{m_{char}}{V_R} C_{C_7H_8}$	S7	
	$C_7H_8 + H_2 \rightarrow C_6H_6 + CH_4$	$r_{11} = 95798 \exp\left(-\frac{79000}{RT}\right) C_{C_6H_6O}$	S3	
	$C_6H_6O \rightarrow CO + 0.4C_{10}H_8 + 0.15C_6H_6 + 0.1CH_4 + 0.75H_2$	$r_{12} = 10^{-2} \exp\left(-\frac{263000}{RT}\right) \frac{m_{char}}{V_R} p_{CH_4}$	S9	
	$CH_4 \rightarrow C + 2H_2$	$r_{13} = 4.8 \times 10^4 \exp\left(-\frac{211000}{RT}\right) p_{H_2O}^{0.51}$	S4	
char and soot gasification	$C_xH_yO_z + (x - y)H_2O \rightarrow xCO + (x - z + y/2)H_2$	$r_{14} = 3 \times 10^{11} \exp\left(-\frac{310000}{RT}\right) \frac{m_{soot}}{V_R} C_{H_2O}$	assumption	Fixed conversion degree justified by fixed temp. and reactor vol. Char ( $C_xH_yO_z$ ) is decomposed into $C$ , $H_2$ , and $O_2$ before combustor. <sup>8</sup>
combustor	$C + O_2 \rightarrow CO_2$ $H_2 + 0.5O_2 \rightarrow H_2O$	$X_C = 95\%$ $X_{H_2} = 100\%$		



Table 6. Name and Description of Material and Energy Streams Used in the Flow Sheets TNEE and FERCO<sup>a</sup>

material and heat streams		description
material and heat stream used in both technologies flow sheets	WET-BIOM	introduction of wet biomass (solid biomass + liquid water)
	DRY-BIOM	dried biomass (with remaining liquid water) to be mixed with fluidization gas and sand
	H <sub>2</sub> O-OUT	water vapor from biomass drying
	TO-GASIF	dry biomass, remaining liquid water, and sand mixed before gasifier injection. Sand is coming from secondary reaction in TNEE (see "SAND" stream) or from combustor in FERCO (see "HOT-SAND")
	TO-2ZR	products of biomass pyrolysis and char gasification (gases, water vapor, tars, and char) + sand
	AFT-2RZ	syngas, water, and tars after cracking in secondary reactions zone + sand
	SYN-GAS	final syngas stream exiting the reactor
	CHAR-COLD-SAND	cold sand and char to combustor (before decomposition of char into C, O <sub>2</sub> , and H <sub>2</sub> )
	C-H <sub>2</sub> -O <sub>2</sub>	stream of C, O <sub>2</sub> , and H <sub>2</sub> after decomposition of char + sand
	AIR	air needed for C and H <sub>2</sub> combustion, flow rate calculated with a Fortran calculator
	AF-COMBU	hot sand with flue gas
	FLUE-GAS	flue gas from combustor after hot sand separation
	HOT-SAND	hot sand separated from flue gas
	1	heat of decomposition of char into C, O <sub>2</sub> and H <sub>2</sub> , injected into the combustor
	Q1	heat required for biomass drying
	Q2	close to 0 (adiabatic reactor). This energy stream is needed to couple Aspen Plus and Fortran subroutine, to close the enthalpy balance (see text).
	Q3	heat (inlet or outlet) to get a temp. equal to 980 °C in combustor
in TNEE flowsheet (presented in Figure 3)	RECY-SG	syngas recycled and used as fluidization agent. RECY-SG mixed with dry biomass and sand before gasifier. RECY-SGA after secondary reaction zone and splitter. Different name but the same stream composition and flow rate.
	RECY-SGA	
	AFT-GASI	gases, water, tars and char from biomass pyrolysis and char gasification + sand
	PYRO-GAS	gases, water vapor and tars from biomass pyrolysis and char gasification separated from sand and char
in FERCO flowsheet (given in the Supporting Information)	SAND	sand coming from secondary reactions zone mixed with dry biomass and recycled syngas before pyrolysis zone
	WATER-IN	introduction of water vapor as fluidization agent

<sup>a</sup>Flow sheets are given in Figure 3 and Supporting Information, respectively.

injected into a separation column called "FIC-CYC1". FIC-CYC1 is a "fictive" cyclone that is not physically a cyclone in the TNEE gasifier. FIC-CYC1 is used to simulate the separation of gases and solid (char + sand) in the dense bed: gases flow from the dense bed to the free-board, and solids from the dense bed to the combustor riser. 5% of the char is assumed to be entrained by gases in the freeboard ( $Y_1 = 0.05$ , defined by relation 1 and in Figure 2).

(d). *Secondary Reactions Zone.* Syngas (and tars) (PYRO-GAS stream) is then mixed with the hot sand coming from the combustor in TNEE flow sheet (Figure 3). Both gaseous and solid streams are then introduced in the secondary reaction zone of the gasifier. The secondary reaction zone is the freeboard of TNEE gasifier with hot sand coming from combustor. Kinetic laws of secondary reactions (given in Table 3) are implemented in an adiabatic plug flow reactor (called 2ND-REAC). After secondary reactions, syngas and sand streams (AFT-2RZ) are then separated by a separation column (CYCL).

Sand is sent from the secondary reaction zone to the dense pyrolysis bed. 14 mass % of the syngas (RECY-SGA) exiting the gasifier is separated and sent after the dryer to be mixed with dry biomass. 86% of the produced syngas (SYN-GAS) exits the TNEE process flow sheet.

(e). *Char Combustion.* Char and cold sand (CHAR-COLD-SAND stream) are separated from the pyrolysis zone by FIC-CYC1 and then introduced in the user block DECOMPO. Char is decomposed into C, O<sub>2</sub>, and H<sub>2</sub>, the yields of which are calculated by a Fortran subroutine from its elemental analysis.

The enthalpy of formation of the char is not equal to the sum of enthalpies of formation of C, H<sub>2</sub>, and O<sub>2</sub>. The heat of decomposition (stream 1) is injected in the combustor (see Figure 3) to close the enthalpy mass balance. This method was taken from Spath et al.<sup>8</sup> and Doherty et al.<sup>65</sup>

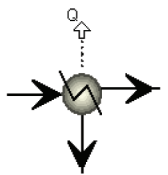
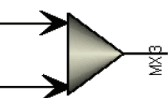
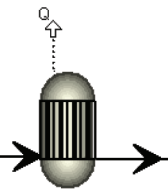
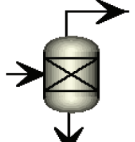
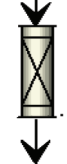
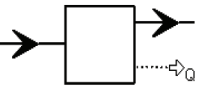
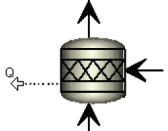
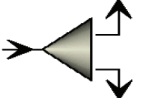
C, H<sub>2</sub>, O<sub>2</sub> and cold sand (C-H<sub>2</sub>-O<sub>2</sub> stream) are sent to a conversion reactor for combustion (COMBUSTO). The conversion degrees for carbon and H<sub>2</sub> oxidation are fixed (see Table 3).

Air flow rate is calculated to achieve these conversion degrees by a Fortran calculator (no air in excess in this paper). Oxidation is conducted in the isothermal conversion reactor set at 980 °C, as in pilot plants. The temperature of the combustor is adjusted as a result of the Q3 heat stream (in Figure 3). Q3 could be positive if an additional heating source is needed to heat the sand flow rate to 980 °C or negative if the heat flux from char oxidation is too high. A discussion on the value of Q3 and on energy efficiency is out of the scope of this paper because this paper only presents the model of the gasifier without heat integration in the whole gasification process.

The temperature of the combustion zone is set to the same temperature as that for the pilot plant for both technologies. The pyrolysis and secondary reaction zones are assumed to be adiabatic. The temperature of the pyrolysis and secondary reactions zones are thus calculated through a complex enthalpy balance that depends mainly on biomass moisture, sand recycling flow rate, enthalpy of reactions, etc. Sand flow rate was adjusted to get the same temperatures in combustion and gasification zones as those in pilot plants (see Table 4). The



Table 7. Different Unit Blocks Used in the Model

Module name	Scheme	Unit Operations	Operating parameters	Comments
Heater		Exchanger	The moisture content of the outlet dry biomass is specified by a calculator.	The heater calculates the energy required to achieve this moisture content (see text).
Mixer		Flow mixer	Temperature (if nothing is specified it takes the temperature of input streams)	-
Yield Reactor		Reactor	Isothermal reactor with temperature calculated by enthalpy balance. Pressure Coupled to a Fortran File	Pyrolysis reactor of biomass and char gasification. These reactions are defined in a Fortran file. This isothermal reactor becomes an adiabatic reactor when the heat (Q2 in figure 3) is set to zero by iterations between Aspen and Fortran files (see text).
Separation column		Separation	Specify the separation degree for each component of the stream	Used for gas-solid separation instead of using a specific cyclone design like in ref. 8, 11, 65.
RPlug		Reactor	For secondary reaction zone. Adiabatic reactor. Pressure	A plug flow reactor for the kinetics of homogeneous and heterogeneous secondary reactions.
User 2		Char decomposition	Char decomposition as a function of its elemental composition.	To decompose the char into C, H <sub>2</sub> and O <sub>2</sub> using a Fortran File based on ref. 8, 65.
Conversion Reactor		Reactor	Temperature Pressure	Used for the combustion of carbon and H <sub>2</sub> with a fixed conversion degree. The heat (Q3) needed to obtain the set temperature (980°C) is calculated.
FSPLIT		Flow divider	Division of the flow rate of the stream.	Used for recycling a fraction of the syngas in TNEE flow sheet

enthalpies of all the compounds (gaseous or solid compounds) and enthalpy balances are calculated by Aspen Plus following the previously presented thermodynamic laws (in section 2.4.2.).

#### 2.4.4. Convergence of the Model and Simulation Outputs.

The convergence of the model is checked for mass and energy balances of each unit blocks (in the simulation final report). Especially for the pyrolysis Fortran file, it should give a closed mass balance: 100% of biomass should be converted in output products from the Fortran File. It is achieved as a result of the correlations followed by char mass yield calculation by difference (as explained in section 2.3.1).

In the simulation options of Aspen Plus, the mass balance error around blocks was checked and its tolerance set at 0.001. For energy balance, the error tolerance (in Flash convergence menu) was set at  $10^{-7}$ . The Newton method was chosen as the convergence options methods.

The main outputs of the model are as follows:

- Temperatures of the gasifier (temperatures of the pyrolysis and secondary reaction zones)
- Composition of syngas (H<sub>2</sub>O, CO, H<sub>2</sub>, CO<sub>2</sub>, CH<sub>4</sub>, C<sub>2</sub>H<sub>4</sub>, C<sub>2</sub>H<sub>6</sub>)
- Concentration of tars (lumped components: benzene, phenol, toluene, and naphthalene)
- Enthalpies of components and mixtures

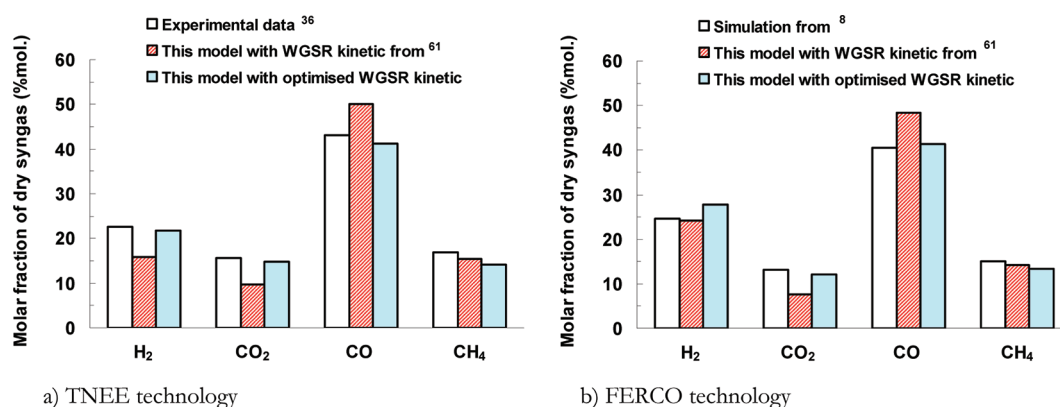


**Figure 4.** Comparison between predicted and experimental molar fraction of dry syngas for (a) TNEE technology and (b) FERCO technology.

- LHV and HHV for conventional components at 0 and 15 °C
- Heat required for drying, incoming heat to the combustor (depending of char flow rate and enthalpy balance to maintain the set temperature of the combustor)
- Gas residence time ( $\tau$ ) in the secondary reaction zone (The volume of the reactor is set as an input, gas residence time depends on syngas volume flow rate.)
- Air flow rate needed for combustion of char (depending on char flow rate and composition from pyrolysis) to achieve a fixed char conversion

### 3. RESULTS AND DISCUSSION

**3.1. Gases Composition.** In the FERCO process model, the pyrolysis zone temperature was adjusted at 870 °C (to be in accordance with ref 8) by adjusting the sand flow rate to 25 kg/s (in agreement with FERCO process,<sup>8,31</sup> 27 kg/s). This temperature is calculated through coupled enthalpy and mass balance, the combustion temperature being set at 982 °C.<sup>8,31</sup> Because of an overall slightly endothermic nature of secondary reactions, the temperature in the secondary reactions zone is 866 °C (slightly lower than 870 °C).

In the TNEE process model, the pyrolyzer temperature was set to 760 °C by adjusting the sand flow to 14.9 kg/s in accordance with the pilot plant.<sup>67</sup> The sand flow rate is lower than for the FERCO process due to higher difference in temperature between the pyrolysis and combustion zones. The sand enters the secondary reactions section at 980 °C and exits from it at 948 °C.

Figure 4 compares the molar fractions of dry gas predicted by the model with two different kinetic constants for the WGSR (see Table 3) and the experimental data from the pilot plants.<sup>8,31,36</sup>

The model gives a good prediction of the mole fractions of CH<sub>4</sub> for both processes. CH<sub>4</sub> is mainly produced by pyrolysis (including primary tar conversion) and then poorly converted in the secondary reaction zones under both technologies conditions. It is a good indicator of the thermal history of gases and tars and of the model accuracy for pyrolysis, including primary and secondary reactions.<sup>51</sup>

CO<sub>2</sub> mole fraction is under predicted by the model and CO mole fraction is overpredicted for both processes with the kinetic constant of WGSR taken from ref 61 (see Table 3) because of a too low conversion degree of CO with this WGSR kinetic. The kinetic constant from ref 61 was chosen because,

according to us, this work is the most advanced one for WGSR gas-phase kinetic.

The gas composition is very sensitive to the WGSR in agreement with ref 26.

Several homogeneous kinetic rates of WGSR presented in Table A (in Appendix A) were tested in our model.<sup>60,68–77</sup> The backward reaction kinetic was calculated (if not given in the references) by using the equilibrium constant<sup>72,74</sup> combined with the forward reaction kinetic.

There are large differences between the kinetic laws of WGSR. Some kinetics mentioned in Table A are either very slow<sup>25,60,61,75–77</sup> or very fast,<sup>68,70,73</sup> which lead to a WGSR already at thermodynamic equilibrium or to very high levels of CO conversion.

A detailed gas-phase mechanism<sup>20,78</sup> was tested under Chemkin independently from Aspen with the mole fractions and thermal conditions occurring in the secondary reaction zones of the two DFB technologies. This detailed model includes 116 species and 811 elementary reactions and was shown to give a very good prediction of the permanent gases evolution over a large range of conditions.<sup>20</sup> The simulation gives a very low CO conversion to CO<sub>2</sub> under the secondary reactors conditions in agreement with the global kinetic law from ref 61.

The same finding has been already mentioned in other works.<sup>26</sup> This discrepancy between experiments and modeling of a too slow WGSR kinetic could be attributed to wall effects or to catalytic effect of the solid materials (sand, char, and ashes) assumed as chemically inert.<sup>26,61,79</sup> For this reason and to evaluate the accuracy of our model for other parameters such as gas flow rate, tar content (etc.), the WGSR pre-exponential factor was optimized for the two technologies on the basis of the kinetic law of Bustamante et al.<sup>61</sup> (see Table 3). The same optimized pre-exponential factor for WGSR was found for both technologies. The optimized kinetic law (given in Table 3) should be suitable for DFB gasifiers with secondary reactions zone temperatures between 850 and 950 °C.

After optimizing the WGSR kinetic constant, H<sub>2</sub>, CO, and CO<sub>2</sub> molar fractions are well predicted by the model for TNEE process. For the FERCO process, H<sub>2</sub> is slightly overpredicted by the model, maybe because of too fast carbon gasification under FERCO conditions.

**3.2. Modeling of Tar Content.** For the TNEE technology, only the total tar content is compared between the experimental and the model prediction (Figure 5) because the experimental composition of tars was not available.

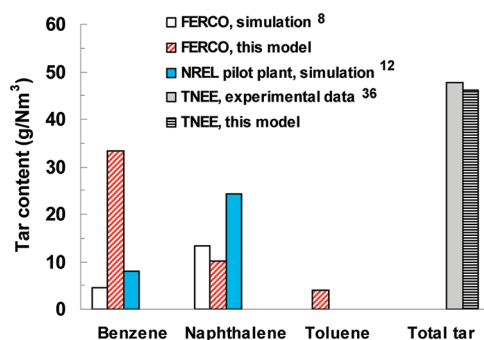


**Figure 5.** Comparison of tar content predictions with experimental data<sup>36</sup> for TNEE process and with two other simulations<sup>8,12</sup> for the FERCO process.

The predicted tar content and mass yield (3.49 mass % tar flow rate/anhydrous biomass flow rate) are in close agreement with the experimental mass fraction (3.80 mass %).<sup>36</sup>

This agreement is mainly due to (i) the pyrolysis correlation that gives tar mass fractions obtained from thermal conditions close to the conditions of the pilot plant and (ii) the detailed kinetic approach for tar conversion with a good selection of the kinetic laws and especially with a very poor catalytic activity of the sand used in the pilot plant.

Figure 5 displays the tar content predicted by the model compared to the tar content determined by the NREL models (from refs 8 and 12) because no detail on the tars composition for the FERCO process was found in the literature.

Table 8 summarizes the experimental conditions and Aspen Plus model adopted in refs 8 and 12, and in this work.

Our model prediction always gives a higher benzene content compared to that provided by NREL correlations.<sup>8</sup> Only a slight difference appears for naphthalene content between Spath et al.<sup>8</sup> correlation and our work. Homogeneous cracking of phenol is mainly complete at the FERCO thermal severity.

Spath et al.<sup>8</sup> assumed in their model that 25 mass % and 75 mass % of tar content is benzene and naphthalene, respectively, which seems less realistic than our pyrolysis correlations. Benzene is the major tar component.<sup>20,80,81</sup>

Tars were analyzed in the FERCO experiments by gravimetric method after separation from quench water and followed by distillation.<sup>31</sup> Tar content was surprisingly independent of reactor temperature between 0.9 and 1.5 mass % on dry biomass basis<sup>31</sup> most probably because of artifacts from the tar analysis method. Kinchin et al.<sup>12</sup> is referred to the new NREL correlations obtained from experiments on the NREL pilot plant.<sup>81</sup> These new correlations have been determined with a more advanced tar analysis methods but on another FB technology in an extensive work.<sup>81</sup> The naphthalene content is under-predicted by our model compared with the new correlation.<sup>12</sup> This discrepancy could not be explained yet. According to our measurement,<sup>51</sup> it seems more realistic to get a higher yield of benzene than of naphthalene. Benzene is much more produced by pyrolysis and secondary reactions and is more stable than naphthalene.<sup>54</sup>

**3.3. Products formation and conversion during secondary reactions.** The conversion ( $X_i$ ) and production ( $Z_i$ ) degrees of a component in the secondary reaction section were defined as follows:

$$X_i = \frac{F_{in,i} - F_{out,i}}{F_{in,i}}$$

**Table 8.** Comparison between Conditions Adopted for Experimental Data and Aspen Plus Model in Refs 8, 12, and This Work

	ref 8	ref 12	this work
experimental results used for the model	Correlations based on run data from the Battelle Columbus Laboratory 9 t/day test facility. The data and correlations for the gasifier can be found in refs 7 and 31.	Results from NREL pilot plant experiments <sup>81</sup> . The effects of 1. feedstock, 2. gasification temp., and 3. steam–biomass mass ratio on char production rate, tar rates, dry gas composition (etc.) were studied.	Lab-scale experimental results for pyrolysis. <sup>50,51</sup> Works from literature for the kinetic of secondary reactions.
definition of the model	Simple raw correlations (mass yields as a function of gasifier temp.) $Y_i = a_i T^2 + b_i T + c_i$ . Global mass yield of tar assuming that 25 mass % of tar is benzene and 75% is naphthalene.	Detailed correlation based on a regression analysis for 18 significant process variables: five ultimate analysis terms (5), four proximate analysis terms (9), gasification temperature (10), steam to biomass ratio (11), residence time (12), three interactions terms (15), and three squared terms (18). Molar fractions of main gases and mass yields of main tar components and char are calculated by the correlations.	A decoupled method to model different gasifier designs. Mass correlations for main pyrolysis products as a function of pyrolysis zone temperature ( $Y_i = a_i T^2 + b_i T + c_i$ ) coupled to a kinetic approach for secondary reactions (water–gas shift, $CH_4$ , and tar gas-phase and catalytic conversion, etc.).

$$Z_i = \frac{F_{\text{out},i} - F_{\text{in},i}}{F_{\text{in},i}}$$

with  $F_{\text{in},i}$  and  $F_{\text{out},i}$  as the molar flow rate (kmol/s) of a component  $i$  at the inlet and outlet of the reactor, respectively.

Table 9 displays the conversion and production degree of the different species.

**Table 9. Conversion and Production Degrees in the Secondary Reaction Section for TNEE and FERCO Reactors with the Optimized Water–Gas Shift Constant (See Table 3)**

component	TNEE (948 °C, $\tau = 1.4$ s)		FERCO (866 °C, $\tau = 1.6$ s)	
	$X_i$	$Z_i$	$X_i$	$Z_i$
conversion/production degrees				
H <sub>2</sub>		0.80		0.68
CO	0.06			0.04
CO <sub>2</sub>		0.71		0.71
C <sub>6</sub> H <sub>6</sub>		0.25		0.04
C <sub>10</sub> H <sub>8</sub>		0.19		0.01
C <sub>6</sub> H <sub>6</sub> O	1		1	
C <sub>7</sub> H <sub>8</sub>	0.68		0.28	
soot	1		1	
char	1		0.18	

The conversion of the small amount of char entrained to the freeboard (5% only of the char produced) is total in the TNEE process with the Barrio et al. kinetic law.<sup>59</sup>

In the TNEE process, H<sub>2</sub> production (12.7 kmol/h) comes at 65% from WGSR and 35% from char (5% entrained) and soot–steam gasification. CO is competitively formed from carbon gasification (4.6 kmol/h) and converted by WGSR (8.3 kmol/h), leading to an overall conversion of CO (6%, Table 9).

In the FERCO process, the entire char produced in the pyrolysis section is entrained in the secondary reaction section under a higher partial pressure of steam. Char has a lower conversion degree (18%, Table 9, 7.4 kmol/h) than in TNEE (100%), which leads to a higher flow rate of H<sub>2</sub> and CO production. H<sub>2</sub> is formed at about 55% from char and soot gasification and 45% from WGSR. CO is consequently more produced by carbon gasification than converted by WGSR. The

rates of char gasification and WGSR are higher in the FERCO process due to a higher steam partial pressure (steam fluidization) and a higher temperature. The higher rate of char gasification compared with WGSR explains the 4% of production degree for CO (instead of 8% conversion in TNEE), although a higher CO<sub>2</sub> production from WGSR is achieved in the FERCO process.

Tar conversion has a minor effect on permanent gas evolution in both processes.

Phenol and toluene mass fractions produced in TNEE pyrolysis section (760 °C) are higher than in the FERCO one (850 °C) due to a lower pyrolysis section temperature in TNEE gasifier. Consequently, the production degrees of benzene and naphthalene from the complete conversion of phenols are much higher in the secondary reaction section of the TNEE gasifier. Toluene conversion is higher in the TNEE process as a result of a higher temperature than that in the FERCO process (better conversion of tar in the hot secondary reaction zone in TNEE, see reactor design in Table 1). Soot–steam gasification is total for both processes with the kinetic law taken from Jess.<sup>54</sup>

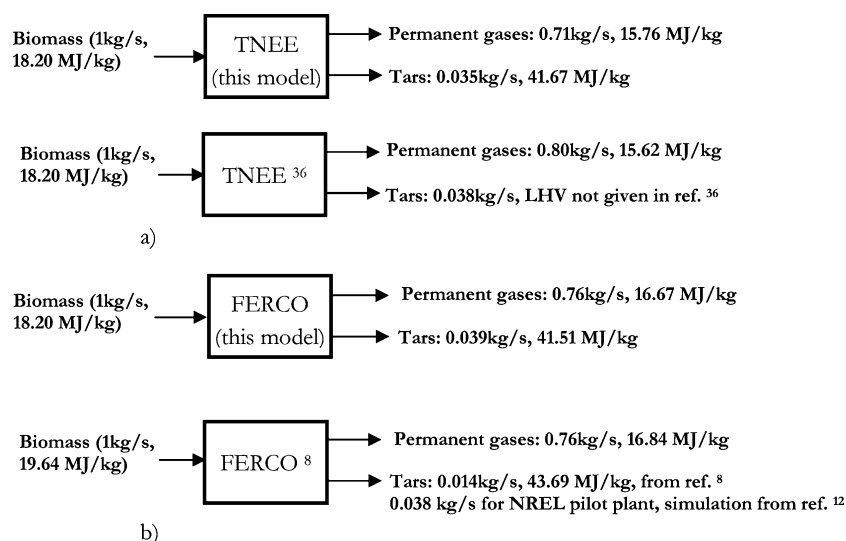
**3.4. Mass Flow Rate and LHV of Permanent Gases and Tars.** The overall energy balances of the process depend on the heat recovery that is not presented in this version of the model. Indeed, this paper gives only the simulation of the gasification section without heat recovery and integration in the entire process. For this reason, permanent gases and tars flow rates and LHVs are more suitable parameters than the cold gas efficiency to evaluate the accuracy of our modeling approach.

Figure 6 shows a simplified scheme of gas and tar mass flow rates and LHVs.

A good agreement is obtained for the total tar flow rate among our model, TNEE data, and the NREL model.<sup>12</sup> Our model gives a lower tar LHV than Spath et al. correlation<sup>8</sup> because of a higher yield in benzene in our case.

The permanent gases flow rate is under predicted compared with the TNEE pilot data, but a mass balance higher than 100% is given for the pilot data,<sup>36</sup> probably due to artifacts on water mass yield determination on the pilot plant.

Permanent gases flow rates and LHV are in very good agreement for the FERCO process between the two modeling



**Figure 6.** Permanent gases and tars flow rate and LHV for the TNEE process (a) and the FERCO process (b).



Table A. Review of WGSR Kinetic Laws (Under Atmospheric Pressure) (kmole, m<sup>3</sup>, K, kJ, Pa)

	rate and equilibrium constant	ref	comment
kinetic with an equilibrium constant	$r = 10^6 \exp\left(-\frac{6370}{T}\right) \times \left(C_{\text{CO}}C_{\text{H}_2\text{O}} - \frac{C_{\text{CO}_2}C_{\text{H}_2}}{K_{\text{eq}}}\right)$ $K_{\text{eq}} = \frac{C_{\text{CO}}C_{\text{H}_2\text{O}}}{C_{\text{CO}_2}C_{\text{H}_2}} = 0.0027 \exp\left(-\frac{3960}{T}\right),$ $T > 1369 \text{ K (equilibrium)}$ $K_{\text{eq}} = 520 \exp\left(-\frac{7230}{T}\right), \quad T < 1369 \text{ K (no equilibrium)}$	25	very slow, i.e. X CO < 1% at 850 °C and $\tau = 1.3 \text{ s}$ .
	$r = 2.78 \times 10^3 \exp\left(-\frac{1510}{T}\right) C_{\text{CO}}C_{\text{H}_2\text{O}},$ $K_{\text{eq}} = 0.0265 \exp\left(-\frac{3968}{T}\right)$	68, 71	very slow at 850 °C and $\tau = 1.3 \text{ s}$
forward reaction kinetics of WGSR without an equilibrium constant	$r = 2.75 \times 10^6 \exp\left(-\frac{83736}{RT}\right) C_{\text{CO}}C_{\text{H}_2\text{O}}$ $r = 2.78 \times 10^3 \exp\left(-\frac{12560}{RT}\right) C_{\text{CO}}C_{\text{H}_2\text{O}}$ $r = 4.28 \times 10^{-12} \exp\left(-\frac{40700}{RT}\right) P_{\text{CO}}P_{\text{H}_2\text{O}}$ $r = 3.75 \times 10^5 \exp\left(-\frac{60690}{RT}\right) C_{\text{CO}}C_{\text{H}_2\text{O}}$ $r = 1.35 \times 10^5 \exp\left(-\frac{102400}{RT}\right) C_{\text{CO}}^{0.5}C_{\text{H}_2\text{O}}$	70 68 69 73 61	very fast, i.e. X CO ~ 100%, at 850 °C and $\tau = 1.3 \text{ s}$
backward reaction kinetics of WGSR without an equilibrium constant	$r = 1.2 \times 10^{13} \exp\left(-\frac{318000}{RT}\right) C_{\text{CO}_2}C_{\text{H}_2}^{0.5}$ $r = 7.6 \times 10^4 \exp\left(-\frac{164200}{RT}\right) C_{\text{CO}_2}C_{\text{H}_2}^{0.33}, \quad T \in 673\text{--}1073 \text{ K}$ $r = 6.4 \times 10^{12} \exp\left(-\frac{326000}{RT}\right) C_{\text{CO}_2}C_{\text{H}_2}^{0.5}, \quad T \in 1023\text{--}1523 \text{ K}$ $r = 1.09 \times 10^7 \exp\left(-\frac{222200}{RT}\right) C_{\text{CO}_2}C_{\text{H}_2}^{0.5}, \quad T \in 1148\text{--}1198 \text{ K}$ $r = 2.3 \times 10^{16} \exp\left(-\frac{397500}{RT}\right) C_{\text{CO}_2}C_{\text{H}_2}^{0.5}, \quad T < 2500 \text{ K}$	77  76 60 75	very slow   very slow, even if quartz bed or inconel wall kinetic laws <sup>61</sup> are considered very slow
equilibrium constant	$K_{\text{eq}} = \exp\left(\frac{4.5778}{T} - 4.33\right)$ $K_{\text{eq}} = \exp\left(\frac{4.1186}{T} - 3.77\right)$	83 70	

approaches: (1) global correlations<sup>12</sup> and (2) pyrolysis correlation coupled with kinetics (this work). This agreement can be explained by a pyrolysis correlation obtained under suitable thermal conditions and by the optimization of WGSR kinetic. Our approach seems to be more general than an overall correlation that can only be used for a given technology. Nevertheless, detailed kinetic data with bed catalytic effects are still needed.

#### 4. CONCLUSION

A methodology is proposed to model a DFB gasifier using Aspen Plus simulator coupled with dedicated Fortran files.

The model is based on decoupling the main phenomena (pyrolysis, char gasification, water–gas shift reaction (WGSR), tar and methane conversion, and char combustion) in different reaction sections under Aspen.

Detailed pyrolysis products mass fractions (permanent gases, water, and 10 tar species lumped in 4 tar model compounds) are given by a correlation implemented in a Fortran file. A semidetailed kinetic mechanism is proposed for secondary reactions. The hypothesis of thermodynamic equilibrium is never taken into account.

Model predictions for methane and tar contents are in agreement with data of pilot plants as a result of the suitability of the pyrolysis correlation and to the semidetailed kinetic

approach for tar conversion. CO, CO<sub>2</sub>, and H<sub>2</sub> mole fractions are very sensitive to the WGSR kinetic. Deeper investigations are needed to predict the kinetic of the WGSR in a FB reactor with coupling between gas-phase and catalytic conversion. Kinetics of C<sub>2</sub>H<sub>4</sub> conversion with potential bed catalytic effect should also be investigated.

The model proposed in this paper could be used to optimize biomass gasifier performances through the design of the DFB technology, the catalyst activity and selectivity, and the operating conditions. Different DFB designs could be modeled under Aspen Plus to optimize the tar cracking zone. This DFB model can be also implemented in a complete process flow sheet for life cycle and techno-economic assessment of the biomass gasification routes.<sup>82</sup> It could be also adapted to model other FB process (combustion, catalytic up-grading) or fluid catalytic cracking process.

## ■ APPENDIX 1. REVIEW OF WATER–GAS SHIFT REACTION (WGSR) KINETIC LAWS

### ■ ASSOCIATED CONTENT

#### ■ Supporting Information

Technical process scheme of the TNEE process, char composition as a function of reactor temperature, kinetic constants calculations for catalytic conversion over char and for carbon steam gasification in the secondary reactions zone, and the Aspen Plus flow sheet of FERCO process. This material is available free of charge via the Internet at <http://pubs.acs.org>.

### ■ AUTHOR INFORMATION

#### Corresponding Author

\*E-mail: [anthony.dufour@ensic.inpl-nancy.fr](mailto:anthony.dufour@ensic.inpl-nancy.fr).

#### Present Address

<sup>†</sup>EDF R&D, Département Mécanique des Fluides, Energies et Environnement, 6 Quai Watier, BP 49, 78400 Chatou, France

#### Notes

The authors declare no competing financial interest.

### ■ ACKNOWLEDGMENTS

Anthony Dufour (CNRS, Nancy) would like to thank Pr. Xavier Deglise (Nancy University) for helpful discussions and data on the TNEE process.

### ■ NOMENCLATURE

$a$ ,  $b$ , and  $c$  = parameters of the correlations for the mass yields ( $Y_i$ ) of the pyrolysis products  $Y_i = aT^2 + bT + c$   
 CHP = combined heat and power  
 $C_i$  = concentration of a component  $i$  (kmol/m<sup>3</sup>)  
 CNRS = French National Centre for Scientific Research  
 $C_p$  = heat capacity (J/(kg K))  
 DCOALIGT = IGT coal density model  
 DFB = dual fluidized bed  
 DFBG = dual fluidized bed gasifier  
 $E_a$  = activation energy (kJ/kmol)  
 FB = fluidized bed  
 FERCO = Battelle high throughput gasification process  
 $F_{in,i}$  = flow rate of a component  $i$  at the inlet of an operating unit (kmol/s)  
 $F_{out,i}$  = flow rate of a component  $i$  at the outlet (kmol/s)  
 HCJ1Boie = coal enthalpy model, based on the Boie's correlation  
 HHV = high heating value (MJ/kg)

HVPR = high velocity pneumatic riser

IGT = Institute of Gas Technology

$K_{eq}$  = Equilibrium constant

$k_i^0$  = Pre-exponential factor of a kinetic constant for a reaction  $i$

$k_i^{*0}$  = Pre-exponential factor of a kinetic constant for a catalytic reaction  $i$  (unit depending on the definition of the rate law)

LHV = lower heating value (MJ kg<sup>-1</sup>)

LVFB = low velocity fluidized bed

$\dot{m}_{char}$  = mass flow rate of char (kg/s)

$m_{char}$  = mass of char (kg)

$M_i$  = molecular weight (kmol/kg)

$m_{soot}$  = mass of soot (kg)

NREL = National Renewable Energy Laboratory

$P_i$  = pressure of specie  $i$  (Pa)

PSR = perfectly stirred reactor

$R$  = ideal gas constant (8.314 kJ/(kmol K))

$r_i$  = rate of a reaction  $i$  (kmol/(m<sup>3</sup> s))

SNG = synthetic natural gas

$T$  = temperature (K)

TNEE = Tunzini Nessi Equipment Companies

$V_R$  = volume of the secondary reactions zone (m<sup>3</sup>)

WGSR = water–gas shift reaction

$X_i$  = conversion degree of a component  $i$  (%)

$Y_1$ ,  $Y_2$ ,  $Y_3$ ,  $Y_4$  = design parameters (ratio of mass flow rates) used to define different dual fluidized bed technologies

$Z_i$  = production degree of a component  $i$  (%)

$\tau$  = residence time of gases in the secondary reactions zone (s)

### ■ REFERENCES

- (1) Hofbauer, H.; Rauch, R. Fluidized bed gasification for biomass combined heat and power production in Güssing. *Euroheat Power, Fernwärme Int.* **2003**, 32 (9), 50–55.
- (2) Rudloff, M. The development and operation of an optimized gasifier for syngas production from biomass. *International Conference on IGCC & Xtl Technologies*, Freiberg, June 16–18, 2005.
- (3) Feldmann, H. F. Conversion of forest residues to a methane-rich gas. *Symposium on Energy from Biomass and Wastes*, Washington D.C., 1978; p 537.
- (4) Corella, J.; Toledo, J. M.; Molina, G. *Ind. Eng. Chem. Res.* **2007**, 46, 6831–6839.
- (5) Göransson, K.; Söderlind, U.; He, J.; Zhang, W. *Renewable Sustainable Energy Rev.* **2011**, 15, 482–492.
- (6) Kaushal, P.; Pröll, T.; Hofbauer, H. *Fuel Process. Technol.* **2008**, 89, 651–659.
- (7) Bain, R. L. *Material and Energy Balances for Methanol from Biomass Using Biomass Gasifiers*, NREL/TP-510-17098; NREL: Golden, CO, 1992.
- (8) Spath, P.; Aden, A.; Eggeman, T.; Ringer, M.; Wallace, B.; Jechura, J. *Biomass to Hydrogen Production Detailed Design and Economics Utilizing the Battelle Columbus Laboratory Indirectly Heated Gasifier*, Technical Report NREL/TP; NREL: Golden, CO, 2005; pp 510–37408.
- (9) Murakami, T.; Xu, G.; Suda, T.; Matsuzawa, Y.; Tani, H.; Fujimori, T. *Fuel* **2007**, 86, 244–255.
- (10) Fryda, L.; Panopoulos, K. D.; Kakaras, E. *Energy Convers. Manage.* **2008**, 49, 281–290.
- (11) Nikoo, M. B.; Mahinpey, N. *Biomass Bioenergy* **2008**, 32, 1245–1254.
- (12) Kinchin, C. M.; Bain, R. L. *Hydrogen Production from Biomass via Indirect Gasification: The Impact of NREL Process Development Unit Gasifier Correlations*, Technical Report NREL/TP; NREL: Golden, CO, 2009; pp 510–44868

- (13) Biagini, E.; Bardi, A.; Pannocchia, G.; Tognotti, L. *Ind. Eng. Chem. Res.* **2009**, *48*, 9028–9033.
- (14) Sadhukhan, J.; Ng, K. S.; Shah, N.; Simons, J. H. *Energy Fuels* **2009**, *23*, 5106–5120.
- (15) Hannula, I.; Kurkela, E. *Bioresour. Technol.* **2010**, *101*, 4608–4615.
- (16) Wang, Y.; Dong, W.; Dong, L.; Yue, J.; Gao, S.; Suda, T.; Xu, G. *Energy Fuels* **2010**, *24*, 2985–2990.
- (17) Baratieri, M.; Baggio, P.; Bosio, B.; Grigante, M.; Longo, G. A. *Appl. Therm. Eng.* **2009**, *29*, 3309–3318.
- (18) Toonssen, R.; Woudstra, N.; Verkooyen, A. H. M. *Int. J. Hydrogen Energy* **2008**, *33*, 4074–4082.
- (19) Paviet, F.; Chazarenc, F.; Tazerout, M. *Int. J. Chem. React. Eng.* **2009**, *7*, A40.
- (20) Dufour, A.; Valin, S.; Castelli, P.; Thiery, S.; Boissonnet, G.; Zoulalian, A.; Glaude, P.-A. *Ind. Eng. Chem. Res.* **2009**, *48*, 6564–6572.
- (21) Jand, N.; Brandani, V.; Foscolo, P. U. *Ind. Eng. Chem. Res.* **2006**, *45*, 834–843.
- (22) Kunii, D.; Levenspiel, O. *Fluidization Engineering*; J. Wiley & Sons: New York, 1969.
- (23) Kersten, S. R. A.; Wang, X.; Prins, W.; van Swaaij, W. P. M. *Ind. Eng. Chem. Res.* **2005**, *44*, 8773–8785.
- (24) Papadikis, K.; Gu, S.; Bridgwater, A. V. *Energy Fuels* **2010**, *24*, 5634–5651.
- (25) Corella, J.; Sanz, A. *Fuel Process. Technol.* **2005**, *86*, 1021–1053.
- (26) Gomez-Barea, A.; Leckner, B. *Prog. Energy Combust. Sci.* **2010**, *36*, 444–509.
- (27) Xu, G.; Murakami, T.; Suda, T.; Matsuzawa, T.; Tani, H. *Ind. Eng. Chem. Res.* **2006**, *45*, 2281–2286.
- (28) Xu, G.; Murakami, T.; Suda, T.; Matsuzawa, T.; Tani, H. *Fuel Process. Technol.* **2009**, *90*, 137–144.
- (29) Dong, L.; Xu, G.; Suda, T.; Murakami, T. *Fuel Process. Technol.* **2010**, *91*, 882–888.
- (30) Deglise, X.; Magne, P.; Donnot, A.; Large, J. P.; Molodtsov, Y.; Lelan, A. Catalytic pyrolysis. In *Biomass for Energy, Industry, and Environment: Proceedings of the 6th International Conference on Biomass*; Grassi, G., Collina, A., Zibetta, H., Eds; Elsevier Applied Science: London, 1991; pp 650–656.
- (31) Feldmann, H. F.; Paisley, M. A.; Appelbaum, H. R.; Taylor, D. R. *Conversion of Forest Residues to a Methane Rich Gas in a High Throughput Gasifier*, Battelle Columbus Laboratories: Columbus, OH, May 1988.
- (32) Hofbauer, H.; Stoiber, H.; Veronik, G.; Gasification of organic material in a novel fluidized bed system. *Proceedings of the 1st SCEJ Symposium on Fluidization*, Tokyo, 1995.
- (33) Pfeifer, C.; Rauch, R.; Hofbauer, H. *Ind. Eng. Chem. Res.* **2004**, *43*, 1634–1640.
- (34) Cen, K. F.; Ni, M. J.; Luo, Z. Y.; Fang, M. X.; Chen, L. M.; Li, X. T. Circulating fluidized bed syngas-steam co-production technique and apparatus. China Patent No. 92100503.2, 1992.
- (35) Schmid, J.; Pröll, T.; Pfeifer, C.; Hofbauer, H. Improvement of gas–solid interaction in dual circulating fluidized bed systems. *Proceedings of the 9th European Conference on Industrial Furnaces and Boilers*, Estoril, Portugal, 2011.
- (36) Gourtay, F.; Nogue, J. C.; Lelan, A.; Déglise, X. Le procédé TNEE de pyrolyse rapide, son application dans l'industrie de la pâte à papier. *Journées Techniques MEI* **87**, 1987.
- (37) Lelan, A.; Magne, P.; Deglise, X. Fast pyrolysis of wood wastes to medium energy gas. *Thermochemical Processing of Biomass*; Bridgwater, A. V., Ed.; Butterworth: London, 1989; p 159.
- (38) Aspen Plus User Models V.7.2; available online: [www.aspentech.com/products/aspen-plus.aspx](http://www.aspentech.com/products/aspen-plus.aspx).
- (39) Wooley, R. J.; Putsch, V. *Development of an ASPEN PLUS Physical Property Database for Biofuels Components*, NREL Technical Report; NREL: Golden, CO, 1996; pp 425–20685.
- (40) Bruni, G.; Solimene, R.; Marzocchella, A.; Salatino, P.; Yates, J. G.; Lettieri, P.; Fiorentino, M. *Powder Technol.* **2002**, *128*, 11–21.
- (41) Cui, H.; Grace, J. R. *Chem. Eng. Sci.* **2007**, *62*, 45–55.
- (42) Kehlenbeck, R.; Yates, J. G.; Di Felice, R.; Hofbauer, H.; Rauch, R. *Ind. Eng. Chem. Res.* **2002**, *41*, 2637–2645.
- (43) Authier, O. Decoupling study of physicochemical phenomena involved inside biomass gasification reactors. Application to a dual fluidized bed. Ph-D thesis, INPL-CNRS-EDF, France, 2010.
- (44) Briens, C. L.; Bergougnou, M. A. *Powder Technol.* **1985**, *42*, 255–262.
- (45) Baron, T.; Briens, C. L.; Galtier, P.; Bergougnou, M. A. *Chem. Eng. Sci.* **1990**, *45*, 2227–2233.
- (46) Briens, C. L.; Bergougnou, M. A.; Baron, T. *Powder Technol.* **1988**, *54*, 183–196.
- (47) Liu, B.; Yang, X.; Song, W.; Lin, W. *Energy Fuels* **2011**, *25*, 1721–1730.
- (48) Evans, R. J.; Milne, T. A. *Energy Fuels* **1987**, *1*, 123–137.
- (49) Dufour, A.; Girods, P.; Masson, E.; Normand, S.; Rogaume, Y.; Zoulalian, A. *J. Chromatogr. A* **2007**, *1164*, 240–247.
- (50) Dufour, A.; Girods, P.; Masson, E.; Rogaume, Y.; Zoulalian, A. *Int. J. Hydrogen Energy* **2009**, *34*, 1726–1734.
- (51) Dufour, A.; Masson, E.; Girods, P.; Rogaume, Y.; Zoulalian, A. *Energy Fuels* **2011**, *25*, 4182–4189.
- (52) Graham, R. G.; Bergougnou, M. A.; Overend, R. P. *J. Anal. Appl. Pyrolysis* **1985**, *6*, 95–135.
- (53) Dufour, A.; Celzard, A.; Quartassi, B.; Broust, F.; Fierro, V.; Zoulalian, A. *Appl. Catal., A* **2009**, *360*, 120–125.
- (54) Jess, A. *Fuel* **1996**, *75*, 1441–1448.
- (55) Morf, P.; Hasler, P.; Nussbaumer, T. *Fuel* **2002**, *81*, 843–853.
- (56) Donnot, A.; Magne, P.; Deglise, X. *J. Anal. Appl. Pyrolysis* **1991**, *21*, 265–280.
- (57) El-Rub, Z. A.; Bramer, E. A.; Brem, G. *Fuel* **2008**, *87*, 2243–2252.
- (58) Dufour, A.; Celzard, A.; Fierro, V.; Martin, E.; Broust, F.; Zoulalian, A. *Appl. Catal., A* **2008**, *346*, 164–173.
- (59) Barrio, M.; Gobel, B.; Risnes, H.; Henriksen, U.; Hustad, J. E.; Sorensen, L. H. Steam gasification of wood char and the effect of hydrogen inhibition on the chemical kinetics. *Progress in Thermochemical Biomass Conversion*; Bridgwater, A. V., Ed.; Blackwell Science: London, 2001; Vol. 32.
- (60) Bustamante, F.; Enick, R. M.; Cugini, A. V.; Killmeyer, R.; Howard, B. H.; Rothenberger, K. S.; Ciocco, M.; Morreale, B. D.; Chattopadhyay, S.; Shi, S. *AIChE J.* **2004**, *50* (5), 1028–1041.
- (61) Bustamante, F.; Enick, R. M.; Killmeyer, R. P.; Howard, B. H.; Rothenberger, K. S.; Cugini, A. V.; Morreale, B. D.; Ciocco, M. V. *AIChE J.* **2005**, *51*, 1440–1454.
- (62) Boie, W. *Energietechnik* **1953**, *3*, 309.
- (63) Raznjevik, K. *Handbook of Thermodynamic Tables and Charts*; Hemisphere Publishing Corporation, McGraw-Hill Book Company: New York, 1976.
- (64) Authier, O.; Ferrer, M.; Mauviel, G.; Khalfi, A.; Lédé, J. *Ind. Eng. Chem. Res.* **2009**, *48*, 4796–4809.
- (65) Doherty, W.; Reynolds, A.; Kennedy, D. *Biomass Bioenergy* **2009**, *33*, 1158–1167.
- (66) EDF R&D, private communication.
- (67) Lelan, A.; Niogret, J.; Magne, P.; Deglise, X. Pyrolyse rapide de déchets lignocellulosiques en lit fluidisé. *4th European Conference on Fluidization*, Toulouse, France, Sept. 18–20, 1985.
- (68) Biba, V.; Macak, J.; Klose, E.; Malecha, J. *Ind. Eng. Chem. Process Des. Dev.* **1978**, *17*, 92–98.
- (69) Desai, P. R. M.S. Thesis, West Virginia University, Morgantown, WV, 1975.
- (70) Jones, W. P.; Lindstedt, R. P. *Combust. Flame* **1988**, *73*, 233–249.
- (71) Parent, J. D.; Katz, S. Equilibrium compositions and enthalpy for the reaction of carbon, oxygen, and steam. *IGT Research Bulletin No. 2*; Institute of Gas Technology: Des Plaines, IL, 1948.
- (72) Yan, H. M.; Heidenreich, C.; Zhang, D. K. *Fuel* **1999**, *78*, 1027–1047.
- (73) Sohn, H. Y.; Braun, R. L. *Ind. Eng. Chem. Process Des. Dev.* **1984**, *23*, 691–696.

- (74) Smith R. J. B.; Loganathany, M.; Shantha, M. S. *Int. J. Chem. React. Eng.* **2010**, 8, Review R4.
- (75) Karim, G. A.; Mohindra, D. A. *J. Inst. Fuel* **1974**, 219.
- (76) Kochubei, V. F.; Moin, F. B. *Kinet. Katal.* **1969**, 10, 992.
- (77) Tingey, G. L. *J. Phys. Chem.* **1966**, 70, 1406–1412.
- (78) Gueniche, H. A.; Glaude, P. A.; Dayma, G.; Fournet, R.; Battin-Leclerc, F. *Combust. Flame* **2006**, 146, 620–634.
- (79) Chen, W. J.; Sheu, F. R.; Savage, R. L. *Fuel Process. Technol.* **1987**, 16, 279–288.
- (80) Carpenter, D. L.; Deutch, S. P.; French, R. J. *Energy Fuels* **2007**, 21, 3036–3043.
- (81) Jablonski, W.; Gaston, K. R.; Nimlos, M. R.; Carpenter, D. L.; Feik, C. J.; Phillips, S. D. *Ind. Eng. Chem. Res.* **2009**, 48, 10691–10701.
- (82) Phillips, S. D.; Tarud, J. K.; Biddy, M. J.; Dutta, A. *Ind. Eng. Chem. Res.* **2011**, 50, 11734–11745.
- (83) Moe, J. M. *Chem. Eng. Prog.* **1962**, 58, 33.